ISSUE: November 2018

Driver IC Subdues Level-Shifting Losses In Active Clamp Flybacks And Other Applications

by Dhruv Chopra, Senior Application Engineer, ON Semiconductor, Phoenix, Ariz.

In a bid to make modern power supplies more compact and efficient, power supply designers are increasingly opting for high-frequency operation (i.e. high-frequency switching). High-frequency operation in a switched-mode power supply (SMPS) can reduce the size of the transformer, increasing the power density of the power supply. High-frequency operation also helps in improving the EMI signature of the power supply. This can result in a lower component count for EMI filtering.

However, there are a few road blocks in implementing high-frequency power supplies. Power switches, transformer core material, leakage losses and switching losses are some of the impediments that are preventing mass production of high-frequency power supplies. With the advent of GaN/SiC technology and continuous development of MOSFET technology, the power switch industry seems to be ready for adoption of high-frequency power supplies. Similarly, transformer core material manufacturers are working tirelessly to innovate high-frequency core materials.

ZVS topologies can eliminate switching losses associated with the power switch. For popular ZVS topologies like LLC half-bridge converters, full-bridge converters, active-clamp flybacks, two-switch forward converters, etc., low−side high−side drivers are needed to perform the function of buffer and level shifter. These devices can drive the gate of the high-side MOSFETs whose source node is a dynamically changing node.

There are inherent losses associated with power switch drivers. In topologies like LLC, half- or full bridge converters, which have a totem-pole structure of power switches, level-shifting losses of the high-side driver are significant. These losses become even worse at higher switching frequencies.

This article focuses on the active clamp flyback (ACF), a relatively new topology that has the potential for very high power density in popular low-power ac adapter applications such as cell phone and laptop chargers. Previously, the use of this topology was held back by the lack of a high-side driver capable of high-frequency operation with low losses. (A lack of suitable magnetics was another obstacle).

In response to this need, ON Semiconductor developed the NCP51530, a 700-V high-side low-side driver for ac−dc power supplies and inverters with very low level-shifting losses. It also has very short propagation delay and low quiescent current. In addition to supporting design of the ACF converters, it also extends the use of superjunction MOSFETs to higher frequencies.

This article describes the application of the NCP51530 driver in a 60-W USB Power Delivery (PD) adapter design based on the ACF. In this design, the NCP51530 is combined with ON Semiconductor's NCP1568, a PWM controller developed specifically for ACF designs. This controller overcomes another problem hindering use of the ACF in ac adapters—excessive losses in standby.

This discussion begins by providing some background on the driver IC and explaining operation of the example ACF-based adapter design. It then compares the performance of the NCP51530 with two industry standard drivers. It presents loss calculations for the NCP51530 in the adapter application. Practical thermal results for the NCP51530 versus the two competitors in an ACF application are then presented. After that, efficiency data for an ACF board using the NCP51530 is compared against efficiency data of the ACF board using the two competitors' parts.

Driver Features

The NCP51530[1] from ON Semiconductor is a 700-V high-side low-side driver for ac−dc power supplies and inverters. This driver IC offers very low propagation delay, and low quiescent and switching current at high frequencies of operation. It also has very low level-shifting losses. This device thus enables highly efficient power supplies operating at high frequencies.

The NCP51530 is offered in two versions, NCP51530A/B. The A version has a typical 50-ns propagation delay, while the B version has a propagation delay of 25 ns. It comes in SOIC8 and DFN10 packages. The SOIC8 package of the device is pin compatible with industry standard alternatives. The NCP51530 has two independent input pins HIN and LIN allowing it to be used in a variety of applications.

This device also includes features wherein, in case of floating input, the logic is still defined. Driver inputs are compatible with both CMOS and TTL logic hence it provides easy interface with analog and digital controllers. The NCP51530 has an undervoltage lockout feature for both high- and low-side drivers, which ensures operation at correct V_{CC} and V_B voltage levels. The output stage of the NCP51530 has 3.5-A/3-A current source/sink capability, which can effectively charge and discharge a 1-nF load in 10 ns.

Active-Clamp Flyback Operation

The active-clamp flyback (ACF) is a variant of the classical flyback topology. The ACF topology is one that utilizes the energy stored in the parasitic to achieve ZVS instead of dissipating the power in snubber circuits. The waveforms resulting from active-clamp operation are typically free of spikes resulting in better EMI than conventional techniques. The ZVS feature allows high-frequency operation of a power converter while achieving high efficiency.

The NCP1568[2] from ON Semiconductor is a highly integrated ac-dc PWM controller designed to implement the active-clamp flyback topology. This controller employs a proprietary variable frequency algorithm to enable ZVS of superjunction MOSFETs or GaN FETs across line, load, and output conditions. The ZVS feature increases power density of a power converter by increasing the operating frequency while achieving high efficiency.

In order to minimize the power loss in ACF operation, as load and input voltage change, the frequency of operation needs to change such that the additional circulating current is kept to a minimum. The negative current needed for ZVS is typically on the order of −0.5 A for superjunction FETs.

Keeping the negative magnetization current relatively constant is accomplished digitally by adjusting the frequency of the oscillator until the SW node fall time is modulated to a predetermined dead time across line and load conditions. A time reference is established in the NCP1568 and an error signal is accumulated based on the time it takes to transition and achieve ZVS.

If the switch-node transitions fast and ZVS occurs before the reference time, then there is more than enough energy to reset the node quickly and therefore the frequency of operation or the off time should be reduced. If the switch-node ZVS occurs coincident with the time reference, no frequency adjustment is necessary. If the ZVS occurs after the reference, the frequency is too high and needs to be reduced to ensure good ZVS.

As expected, this algorithm works much more efficiently with a high-side driver with fast propagation delays. With this algorithm, a driver with slower propagation delay will result in lower-frequency operation as compared to a faster propagation delay driver. This results in inefficient operation of the overall system and higher losses.

A top level schematic of the ACF board using the NCP1568 and NCP51530 is shown in Fig. 1. This schematic was implemented in a 60-W, universal-input, 20-V output power supply[3]. This featured power supply uses ON Semiconductor's NCP1568 PWM controller, NCP51530 high-side low-side driver, NCP4305 synchronous rectifier

(SR) controller and FDMS86202 SR FET. This converter employs variable frequency operation with ACF operation ranging from 200 kHz to 425 kHz. Typical ACF waveforms are shown in Fig. 2.

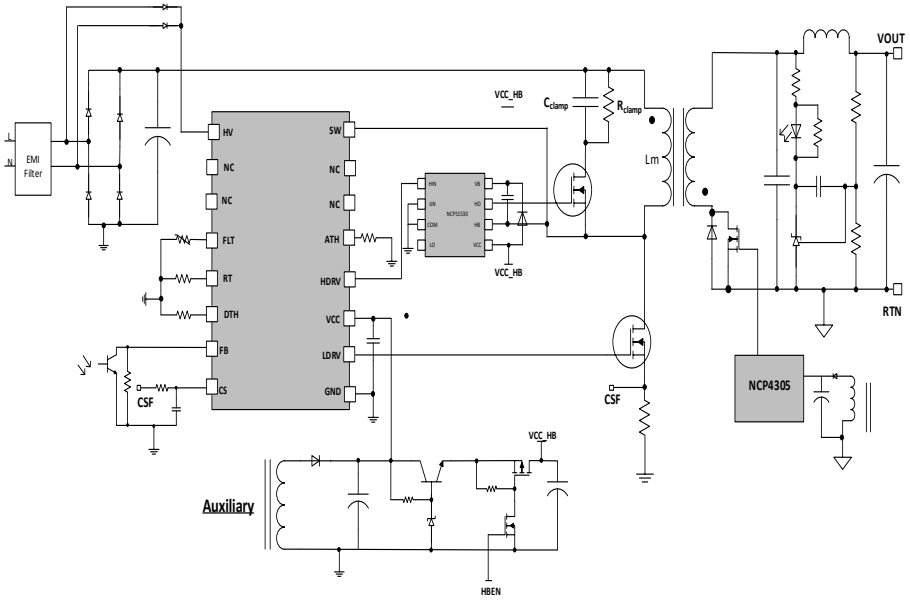

Fig. 1. An ACF converter using the NCP51530 driver and the NCP1568 controller.

Fig. 2. Waveforms produced by the ACF converter shown in Fig 1. Blue trace = switch node waveform, yellow trace = low-side drive signal and green trace = high-side drive signal.

Loss Calculations

In this section, we calculate power dissipation of the NCP51530 driver in an ACF application using the NCP1568 controller. Total power losses in a driver can be broadly divided into static and dynamic power losses.[4] Static power losses are caused by the bias current required for the device operation. Dynamic losses are due to the switching characteristic of the device. Dynamic losses can be further divided into losses caused by charging and discharging of the gate of the external FET and losses caused by charging and discharging of level-shifter capacitance.

The total power dissipation of the NCP51530 can be calculated step by step as follows.

1. Static power loss of the device (excluding drivers) while switching at an appropriate frequency.

$$P_{operating} = V_{boot} * I_{BO} + V_{CC} * I_{CCO} = 14V * 0.4mA + 15V * 0.4mA = 11.6\,mW$$

where I_{BO} is the operating current for the high-side driver and I_{CCO} is the operating current for the low-side driver.

2. Power loss of driving the external FET

This loss is due to charging and discharging of the gate capacitors of the external FETs. Since in this ACF application only one external FET is driven by the NCP51530 we are taking into account the power loss of driving only one MOSFET. In the case where the NCP51530 is used to drive both high- and low-side FETs, the power loss of charging and discharging the gates of two external MOSFET devices has to be included.

$$P_{drivers} = \left(Q_{gs} * V_{boot}\right) * f = (4\,nC * 14\,V) * 425\,kHz = 23.8\,mW$$

where Q_{gs} is gate-to-source charge of the MOSFET, V_{boot} is the high-side bias supply voltage and f is the frequency of operation.

3. Level shifting losses[4]

Whenever the high-side switch is turned off, it causes a current to flow into the level-shifting circuit to charge the ldmos1 capacitance. This current comes from the high-voltage bus through the power device and the bootstrap capacitor. On the other hand when the high-side switch is turned on, it causes a current to flow from V_{CC} through the boot diode into the level-shifting circuit. The losses due to this current flow are calculated as follows.

$$P_{levelshifting} = (V_{SW} + V_{boot}) * Q_{ls} * f = 415V * 0.5\,nC * 425\,kHz = 88.2\,mW$$

where Vsw is the rail voltage, Q_{ls} is the substrate charge on the level shifter, V_{boot} is the high-side bias supply and f is the frequency of operation.

4. Losses due to charging and discharging of p-well capacitance[4]

In a half-bridge-type power circuit, every time the switch node swings between rail and ground level, the well capacitance is charged and discharged. Current flows from the bulk voltage through the high-side external device and epi resistance to charge the well capacitance. The discharge path of this capacitance is through the low-side device and the epi resistance of the driver. Most of these losses occur outside the high-side low-side

driver since the epi resistance is much smaller that the internal resistance of the power devices. Hence these losses are not considered as losses inside the high-side low-side driver.

$$P_{Csub} = (V_{SW}) * Q_{Cwell} * f$$

where Vsw is the rail voltage, Q_{Cwell} is the substrate charge on the capacitor well on the switch node and f is the frequency of operation. A numerical value for P_{Csub} is not shown here because the value for Q_{Cwell} is still under review.

5. Total power loss inside driver

The total power loss in the driver is the sum of external FET driving losses, static losses and level-shifting losses. The losses due to charging and discharging of well capacitance C_{well} are not considered here since most of these losses are inside the MOSFET rather than driver. These losses however would affect the system efficiency.

$$P_{total} = P_{drivers} + P_{operating} + P_{levelshifting} = 12mW + 17mW + 88mW = 117\ mW$$

6. Junction temperature increase

$$t_j = R_{\theta JA} * P_{total} = 183 * 0.117\ = 21.5\ °C$$

where t_j is the junction temperature, $R_{\theta JA}$ is the thermal resistance and P_{total} is the total power loss in the device..

Comparison With Competing Solutions

Two competitors, which are industry standard parts used in similar applications as the NCP51530 and with the same package as the NCP51530 were selected for comparison. They were then tested in the same ACF EVB setup as the NCP51530. There were two comparisons made—the thermal data of the three driver ICs under exactly the same conditions, and the efficiency of ACF board with the three driver ICs.

Thermal Results

The NCP1568 uses a proprietary variable-frequency algorithm to enable ZVS under all operating conditions. As explained above, the different propagation delays of the three driver devices result in different operating frequencies under the same load conditions. For the sake of fair comparison, this algorithm was turned off for the thermal comparison of the three devices. The EVB was configured to run at a constant frequency of 425 kHz. The thermal data for the three devices was taken at 115-Vac input and 1-A output load.

Table 1 presents the maximum and minimum temperatures of the driver devices in the ACF EVB. Figs. 3, 4 and 5 show the thermal images of the NCP51530, competitor 1 and competitor 2 devices, respectively, running in the application. As can be seen in the thermal images, the NCP51530 runs much cooler compared to the two industry-standard competitors.

At 425-kHz operation, the NCP51530 temperature is just around 50°C. Meanwhile, the temperature on competitors 1 and 2 was found to be above 90°C. The difference in performance will become even more prominent at higher switching frequencies. This is because level-shifting losses are one of the most important sources of loss in the high-side low-side driver-loss mechanism. The NCP51530's exceptional thermal performance allows it to be used in high density boards.

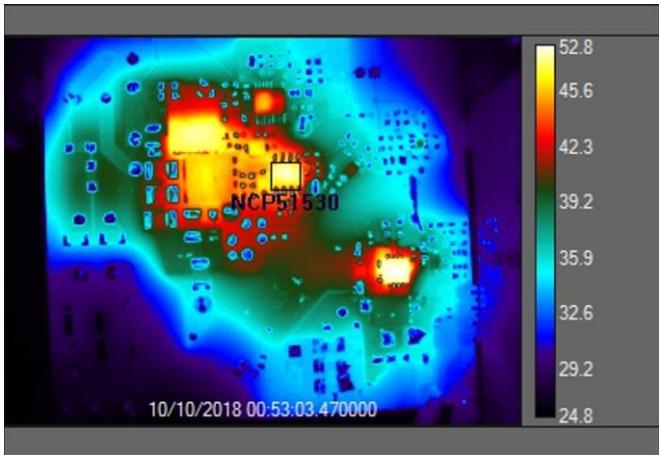

Fig. 3. Thermal image of the ACF operating with the NCP51530 driver.

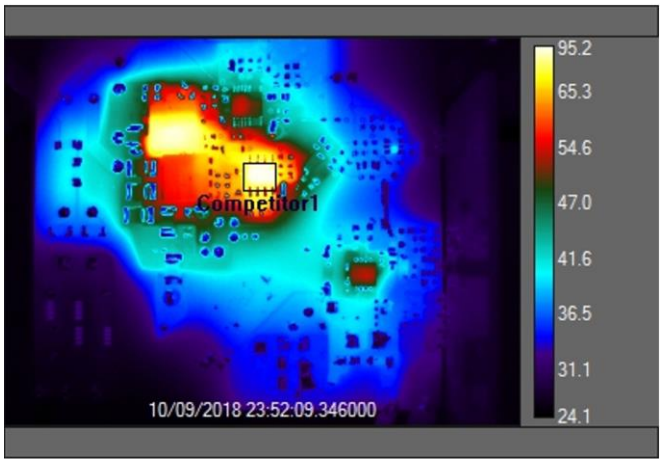

Fig. 4. Thermal image of the ACF operating with Competitor 1's driver.

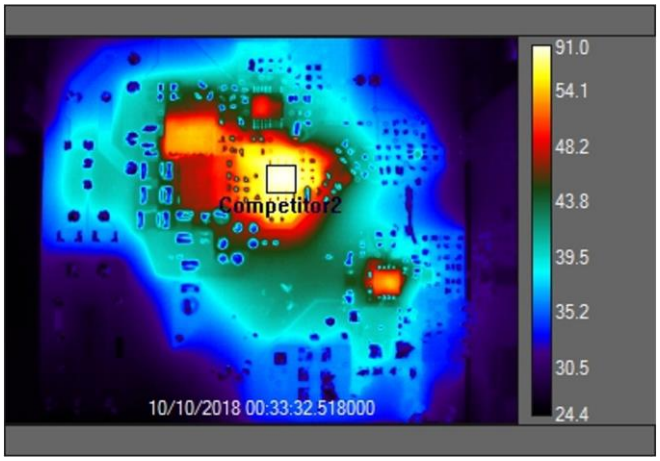

Fig. 5. Thermal image of the ACF operating with Competitor 2's driver.

Table 1. Temperature measurements for the three devices operating in the ACF EVB.

Device	Max temp (°C)	Mean temp (°C)
NCP51530	52.58	49.23
Competitor 1	95.02	83.22
Competitor 2	90.95	80.26

Efficiency Comparison

Efficiency data for the ACF board with three driver devices was taken with the ZVS algorithm turned on. Efficiency was measured at both 115-Vac and 230-Vac input and four load points of 0.5 A, 1 A, 1.5 A and 2 A. The data is presented in Tables 2 and 3, and in Figs. 6 and 7.

The difference in efficiency between the NCP51530 and the competitors is more than 1% at 40-W load and more than 2% at lower loads. This is well illustrated in the two graphs in Figs. 6 and 7, respectively. At lower load points, the NCP1568 operates at higher frequencies and as shown above at higher frequencies the loss difference between the NCP51530 and competitors becomes greater. This is why the performance of the NCP51530 in the ACF EVB at lower loads is even better than at higher loads.

This improvement in efficiency is a direct result of lower level-shifting and C-well charging and discharging losses. While, the effect of lower level-shifting losses can be seen directly in the thermal data, the combined effect of level shifting and C–well charging and discharging losses results in improved system efficiency.

Table 2. 115-Vac efficiency data for the ACF EVB.

	Efficiency (%)		
Output current (A)	NCP51530	Competitor 1	Competitor 2
2	92.96	91.99	92.31
1.5	92.59	91.26	91.76
1	91.00	89.49	89.89
0.5	86.08	83.71	83.98

Table 3. 230-VAC efficiency data for the ACF EVB.

	Efficiency (%)		
Output current (A)	NCP51530	Competitor 1	Competitor 2
2	92.53	91.57	91.36
1.5	91.37	89.91	89.94
1	88.69	86.63	86.63
0.5	83.23	78.02	78.19

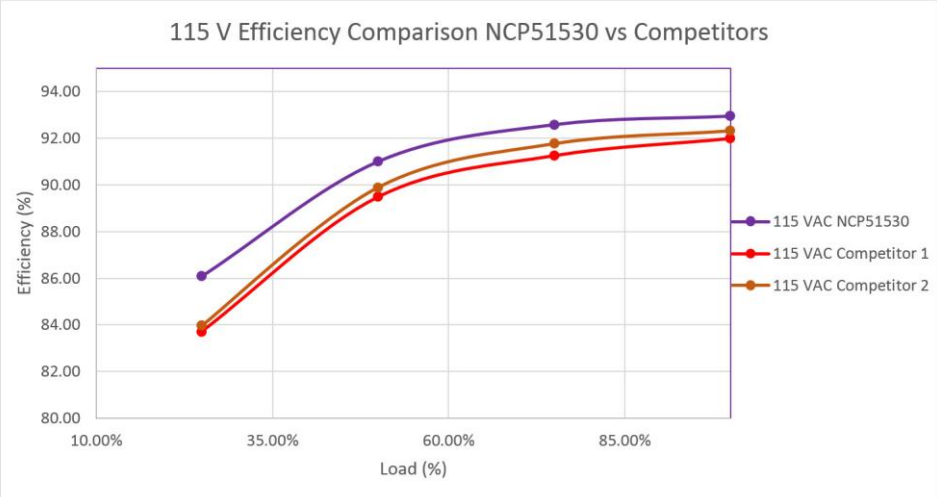

Fig. 6. Efficiency of the NCP51530 vs. competitors in the ACF EVB at 115-Vac input.

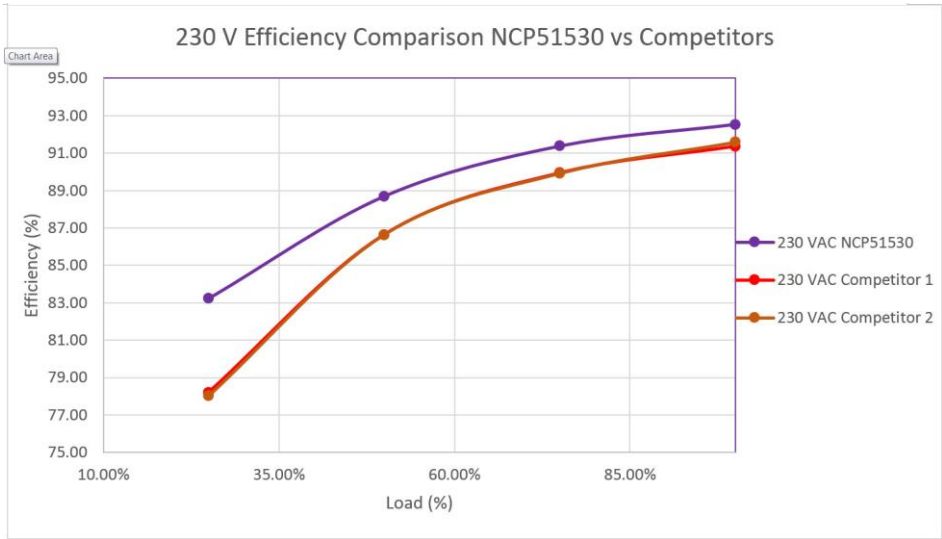

Fig. 7. Efficiency of the NCP51530 vs. competitors in the ACF EVB at 230-Vac input.

Conclusion

The thermal and efficiency data show that the NCP51530 has much better performance than the two industry standard parts. In the thermal data comparison, the maximum NCP51530 device temperature was observed to be 50°C while the competing device temperatures were observed to be above 90°C at the same line and load conditions. The ACF board using NCP51530 was found to be around 1% more efficient at full load compared to the ACF board using the two competitor devices. The NCP51530 also has very fast propagation delays and thus optimizes ACF operation.

These results demonstrate that the NCP51530 is a high-performance device and suitable for high-frequency applications. Higher frequency usually results in smaller transformer size, hence a higher density power board design. Also the NCP51530's exceptional thermal performance allows it to be used in high density boards without increasing the thermal signature of the board.

The NCP51530 enables many high-frequency topologies which previously needed more-expensive drive solutions such as pulse transformers. As a result, this device will help to drive high-frequency topologies with ultra high density to market which were previously on the backburner due to lack of an efficient high-side low-side driver.

References

1. NCP51530 data sheet
2. NCP1568 landing page
3. NCP1568 EVB landing page
4. "HV Floating MOS-Gate Driver ICs" International Rectifier application note AN-978.

About The Author

Dhruv Chopra currently works as senior applications engineer for the AC-DC Group at ON Semiconductor. Dhruv joined ON Semiconductor as an applications engineer in December 2013. Previously, Dhruv was an R&D engineer at Tribi Systems Pvt. Ltd, Bangalore, India. Dhruv holds a masters in science (MS) in electrical engineering from Arizona State University and a bachelors of technology (ECE) from GGSIP University India.

For more information on flyback converter design, see How2Power's Design Guide, locate the Topology category and select Flyback.